FEM-based reduced-order model for steady-state skin-effect analysis in lossy lines

Francesco Bertazzi, Francesco Carbonera, Michele Goano, and Giovanni Ghione

Abstract—**A quasi-static finite element technique is proposed for the accurate and efficient computation of the frequency-dependent characteristic parameters of lossy transmission lines having electrodes of arbitrary cross-section on multi-layered, planar or non-planar substrates. A novel formulation of the magneto-quasi-static problem is combined with a robust fast frequency-sweep technique based on the numerical generation of problem-matched basis functions. The proposed technique enables to accurately model the frequency-dependent penetration of electromagnetic fields inside lossy conductors with a reduced set of problem-specific functions.**

Extensive comparisons are provided between state-of-the-art full-wave finite element method and the present technique: excellent agreement is demonstrated with the full-wave solution, at a fraction of its computational cost.

Keywords—**Coplanar waveguides, skin-effect, model reduction.**

I. INTRODUCTION

The design of microwave integrated circuits demands accurate modeling tools. General models are necessary to deal with arbitrary cross sections, anisotropic substrates with dielectric losses, and metallic regions of finite conductivity whose thickness may be smaller or larger than the skin penetration depth within the frequency range of interest. Among suitable analysis techniques, the finite element method (FEM) probably is the most flexible and powerful.

In the conventional full-wave FEM, the transverse component of the electric (magnetic) field is expanded with curl-conforming vector elements of order p [1], whereas the longitudinal component is represented with conventional scalar elements of order $p+1$. Once the simulation region has been divided into a number of such hybrid elements, application of Galerkin's criterion to the vector wave equation yields a sparse generalized eigenvalue problem, whose solutions are the complex propagation constants of the guided modes of the structure [2–5]. The resulting large-scale eigenvalue problem may be efficiently solved via the implicitly restarted Arnoldi method [6]. Nevertheless, the full-wave approach is still too computationally expensive for the direct inclusion in CAD tools for circuit analysis and design. In the present paper, we propose a fast and accurate quasi-static FEM technique for the extraction of the frequency-dependent characteristic parameters of lossy inhomogeneous transmission lines.

When quasi-TEM wave propagation is assumed, the computation of the electric field reduces to the electrostatic problem governed by Laplace's equation, and the vector magnetic potential has only one component along the propagation direction, which satisfies the well known integrodifferential equation governing the 2-D eddy-current problem [7]. In the present paper, the skin-effect problem is solved via a superposition approach. In contrast with the integrodifferential formulation, our approach leads to a sparse finite element equation. Although modal dispersion is negligible for quasi-TEM lines, skin-effect losses are responsible for strong dispersion from the low frequency RC range to the skin-effect LC regime. Since we are concerned with the computation of the circuit parameters of the line versus frequency, we have developed a robust fast frequency-sweep technique based on the numerical generation of problem-specific basis functions [8], thus drastically reducing the computation time. The proposed approach preserves the sparsity of the problem, and allows for a drastic reduction of the number of basis functions without loss of accuracy. The new technique has been validated against full-wave analysis: excellent agreement is demonstrated with the full-wave solution, as long as modal dispersion is negligible.

The paper is structured as follows. In Section II, the novel formulation of the eddy-current problem is derived. In Section III, problem-matched basis functions are numerically generated via the singular value decomposition (SVD). Two examples, a cylindrical wire and a ridge-type coplanar waveguide for electro-optic applications, are discussed in Section V. Some concluding remarks are finally reported in Section VI.

II. EDDY-CURRENT FORMULATION

Consider a microwave transmission line consisting of an active conductor and a number of ground electrodes, embedded in a lossy, non-homogeneous dielectric medium, characterized by diagonal permittivity and permeability tensors $[\tilde{\epsilon}]$, $[\mu]$. Dielectric losses are included in the imaginary part of the permittivity tensor. Let us assume that the line is uniform along the z-axis, and let the electrodes have arbitrary cross-sections Ω_k and finite conductivity σ.

In the present formulation, a vector potential $\vec{A}$ and a scalar potential ϕ are chosen as unknown variables. They are defined through the electric and magnetic fields as

$$\begin{cases} \vec{B} = \nabla \times \vec{A} \\ \vec{E} = -j\omega\vec{A} - \nabla\phi. \end{cases} \tag{1}$$

From potential theory, it is well known that the vector potential $\vec{A}$ is not unique unless a gauge condition is imposed. If the Lorentz condition is used, an inhomogeneous Helmholtz equation for the magnetic potential $\vec{A}$ is derived [9]

$$\nabla^2\vec{A} + \omega^2[\mu][\tilde{\epsilon}]\vec{A} = -[\mu]\vec{J}_s. \tag{2}$$

When quasi-TEM wave propagation is assumed, the source current density $\vec{J}_s$ has only one component along the z-direction, and is constant over each conductor

$$\vec{J}_s = J_k^{(s)}\hat{z} \quad \forall (x,y) \in \Omega_k \tag{3}$$

This research was partially supported by CNR (Italian National Research Council) through the MADESS II project.

The authors are with the Dipartimento di Elettronica, Politecnico di Torino, corso Duca degli Abruzzi 24, I-10129 Torino, Italy. E-mail: ghione@polito.it.

0-7803-7239-5/02/$10.00 © 2002 IEEE

where $J_k^{(s)}$ are the source current density values on the electrodes. Thus, neglecting displacement currents, (2) simplifies to

$$\begin{aligned} \nabla^2 A - j\omega\mu\sigma A &= -\mu J_k^{(s)} && \forall\,(x,y) \in \Omega_k \\ \nabla^2 A &= 0 && \forall\,(x,y) \in \Omega_d \end{aligned} \quad (4)$$

where Ω_d denotes the dielectric region outside the metallic materials. In equation (4) the unknowns are the potential function $A(x,y)$ and the frequency-dependent source values $J_k^{(s)}$. The total average current density $J_k = I_k/S_k$ over each electrode may be computed as

$$J_k = J_k^{(s)} - j\omega\sigma\tilde{A}_k \quad (5)$$

where $\tilde{A}_k$ is an average value of the magnetic potential over the k-th electrode cross-section

$$\tilde{A}_k = \frac{1}{S_k}\iint_{\Omega_k} A(x,y)\mathrm{d}x\,\mathrm{d}y. \quad (6)$$

Solving (5) for $J_k^{(s)}$ and substituting into (4), we get the well-known integrodifferential equation governing the 2-D eddy-current problem [7, 10]

$$\begin{aligned} \nabla^2 A - j\omega\mu\sigma A + j\omega\mu\sigma\tilde{A}_k &= -\mu J_k && \forall\,(x,y) \in \Omega_k \\ \nabla^2 A &= 0 && \forall\,(x,y) \in \Omega_d. \end{aligned} \quad (7)$$

Equation (7) contains only the unknown A, and the forcing terms are the total currents $I_k = J_k S_k$ flowing in the conductors.

The finite element discretization of the integrodifferential equation (7) would lead to a sparse coefficient matrix, if not for the dense contribution deriving from the average values $\tilde{A}_k$. In the integrodifferential approach, the unknowns $J_k^{(s)}$ are eliminated at the expense of the matrix sparsity. However, notice that if the source values $J_k^{(s)}$ were known a priori, one could directly solve equation (4) for A. The basic idea is to represent the magnetic potential A as the superposition of two linearly independent solutions of equation (4), obtained by setting unit source current density in the active electrode and in the ground conductors successively

$$A(x,y) = \sum_{m=1}^{2} C_m A_m(x,y). \quad (8)$$

Owing to the linearity of the operators in (7), equation (5) may be expanded as

$$\begin{aligned} I &= (1 - j\omega\sigma\tilde{A}_{h1})S_h C_1 + (-j\omega\sigma\tilde{A}_{h2})S_h C_2 \\ -I &= \sum_{k\neq h}(-j\omega\sigma\tilde{A}_{k1})S_k C_1 + \sum_{k\neq h}(1 - j\omega\sigma\tilde{A}_{k2})S_k C_2 \end{aligned} \quad (9)$$

where I is the total current carried by the active electrode (h-th electrode) which flows back in the ground conductors, and

$$\tilde{A}_{km} = \frac{1}{S_k}\iint_{\Omega_k} A_m(x,y)\mathrm{d}x\,\mathrm{d}y \quad (10)$$

Once equation (9) has been solved for the coefficients C_m, the unknown potential A may be derived from the superposition principle (8).

After a suitable choice of the basis functions, the application of Galerkin's procedure to the equation (4) yields the following system of matrix equations [7]

$$(\boldsymbol{S} - j\omega\sigma\,\boldsymbol{T})\cdot\boldsymbol{A}_m = \boldsymbol{J}_m^{(s)}, \quad m = 1,2 \quad (11)$$

where $\boldsymbol{J}_m^{(s)}$ originates from the imposed source current density distribution on the electrodes, and $\boldsymbol{S}$, $\boldsymbol{T}$ are sparse matrices, whose analytic expressions can be found in [7], if Lagrange polynomials are used to expand the unknown. Notice that the finite element equation (11) may be efficiently solved for any source current distribution, once a sparse factorization of its coefficient matrix has been obtained. The solution vector $\boldsymbol{A}$ induced by the imposed currents J_k may be derived from the superposition principle (8) and (9).

III. Reduced-order model

Since we are concerned with the computation of the circuit parameters of a line versus frequency, the analysis should be repeated for many frequency sampling points in the range of interest. Recently, a novel technique for the numerical generation of an orthonormalized set of problem-matched basis functions has been introduced with application to the scattering problem [8]. The basic idea is the generation of problem-specific basis functions based on the exact analysis in a few frequency points chosen in the range of interest. These basis functions are extremely efficient in the representation of the unknown, thus drastically reducing the CPU-time. In this paper, the concept of problem-matched basis functions is applied to eddy-currents computations.

We evaluate the potential function A, via the standard FEM, at P frequency points $\omega = \omega_1 \cdots \omega_P$ chosen in the band of interest. The FEM solution vectors $\boldsymbol{A}(\omega_p)$ are arranged column-wise in a matrix $\boldsymbol{X}$, which is then subjected to the economy-size Singular Value Decomposition (thin SVD) [11]:

$$\boldsymbol{X} = \boldsymbol{U}\,\boldsymbol{\Sigma}\,\boldsymbol{V}^{\dagger}. \quad (12)$$

The columns of $\boldsymbol{U}$ are the singular vectors, and the diagonal elements of matrix $\boldsymbol{\Sigma}$ are the corresponding singular values. The singular values measure the significance of each singular vector in the representation of the unknown. Since they range over several orders of magnitude, not all of them are needed to get accurate results [3]. Let then $Q \leq P$ be the number of singular vectors assumed to be adequate to represent the unknown. The selected singular vectors define a set of problem-matched basis functions of the subspace Ξ that contains the potential representation, at least in the band of interest. The restriction of the large-scale equation (11) in the subspace Ξ yields the reduced-order model

$$\left(\boldsymbol{U}_Q^{\dagger}\boldsymbol{S}\boldsymbol{U}_Q - j\omega\sigma\,\boldsymbol{U}_Q^{\dagger}\boldsymbol{T}\boldsymbol{U}_Q\right)\hat{\boldsymbol{A}}_m = \boldsymbol{U}_Q^{\dagger}\boldsymbol{J}_m^{(s)} \quad (13)$$

where matrix $\boldsymbol{U}_Q$ consists of the first Q singular vectors selected. Equation (13) has size $Q \times Q$, and may be easily solved

by a direct method for each frequency value. Moreover, by inspection of the dynamic range of the singular values, the accuracy level of the procedure can be controlled: if the singular values have a small dynamic range, not enough information has been acquired, and the frequency sampling rate should be increased.

IV. Evaluation of the Quasi-TEM Line Parameters

The evaluation of the quasi-TEM line parameters requires the solution of the electrostatic problem for the line p.u.l. parallel admittance and the solution of the eddy-current problem for the line p.u.l. series impedance, as discussed in Section II. The finite element discretization of Laplace's equation yields the matrix equation $\boldsymbol{K}\,\boldsymbol{\phi} = \boldsymbol{q}$, where $\boldsymbol{K}$ is a sparse matrix and the column vector $\boldsymbol{q}$ originates from the applied voltage V_a and corresponds to the surface charge distribution on the electrodes [5]. Since dielectric losses are described by a frequency-independent loss tangent, also Laplace's equation does not depend on frequency. The p.u.l. admittance $\mathcal{Y} = \mathcal{G} + j\omega\mathcal{C}$ may be computed from the complex electrostatic stored energy as

$$(\mathcal{G} + j\omega\mathcal{C})\, V_a^2 = j\omega(\boldsymbol{\phi}^{\dagger}\, \boldsymbol{K}\, \boldsymbol{\phi}). \tag{14}$$

Notice that the p.u.l. conductance $\mathcal{G}$ is a linear function of frequency. If, on the other hand, dielectric losses are modeled as a constant conductivity, Laplace's equation becomes frequency-dependent, requiring fast-sweep solution techniques similar to those described in Section III.

The p.u.l. impedance $\mathcal{Z} = \mathcal{R} + j\omega\mathcal{L}$ may be computed from

$$-\frac{dV}{dz} = (C_1 - C_2)/\sigma = (\mathcal{R} + j\omega\mathcal{L})I \tag{15}$$

Notice that, once the set of problem-matched basis functions has been defined, the evaluation of the average values $\tilde{A}_{km}$ and all postprocessing computations may be performed directly in the reduced-order representation.

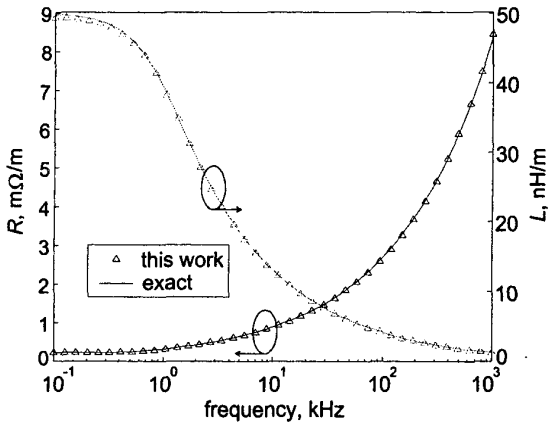

Fig. 1. Comparison between the p.u.l. resistance $\mathcal{R}$ and p.u.l. internal inductance $\mathcal{L}_i$ versus frequency of a copper cylindrical wire (radius $r = 5$ mm, conductivity $\sigma = 5.8 \times 10^7$ S/m) computed analytically and with the present numerical approach.

V. Results

In order to show the effectiveness of the proposed numerical technique, we analyze two different structures, a cylindrical wire and a coplanar waveguide on a lithium niobate substrate with application to electro-optic devices. Excellent agreement is demonstrated with the full-wave solution, at about one tenth of its computational cost.

A. Cylindrical wire

We consider a copper cylindrical conductor with radius $r = 5$ mm, and conductivity $\sigma = 5.8 \times 10^7$ S/m. We have computed the potential function A at the frequency points $f = 0.1, 1, 10, 100, 1000$ kHz. The singular values range over five orders of magnitude, which confirms that the frequency sampling rate is adequate to represent the solution over the selected frequency range. Fig. 1 compares the series parameters $\mathcal{R}$ and $\mathcal{L}_i$ evaluated with their exact analytical expressions [9] and with the present quasi-static FEM approach with $Q = 5$ problem-matched basis functions (all the singular vectors have been retained). The p.u.l. resistance $\mathcal{R}$ asymptotically behaves as $\sqrt{f}$ in the skin-effect regime, and reaches the DC limit according to a complex and conductor shape-dependent frequency behaviour. The p.u.l. internal inductance $\mathcal{L}_i$ has been computed integrating the magnetic energy over the conductor cross-section [12]. As it can be observed, the frequency variations of the circuit parameters are represented without loss of accuracy with just $Q = 5$ problem-matched basis functions.

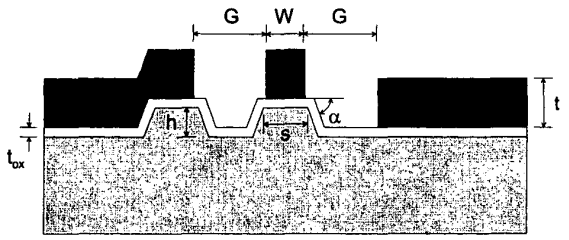

Fig. 2. Cross section of a ridge-type CPW. The geometrical parameters are: $t = 10\,\mu$m, $W = 8\,\mu$m, $G = 15\,\mu$m, $t_{ox} = 1.2\,\mu$m, $h = 3.3\,\mu$m, $s = 9\,\mu$m, $\alpha = 70$ degrees.

B. Ridge modulator

State-of-the-art electro-optic modulators on $LiNbO_3$ substrates are now reaching bandwith performances in excess of 40 GHz with driving voltages around 5 V. The design and optimization of such structures demand precise modeling of their microwave propagation characteristics because of the contrasting requirements in terms of velocity matching, low microwave attenuation, and good superposition between the optical and the microwave fields.

Recently, a novel ridge-type lithium niobate modulator has been introduced to achieve low drive voltage and broad band operation [13, 14]. In this structure (see Fig. 2), synchronous coupling with the optical signal is achieved removing the high dielectric constant lithium niobate around the center conductor, and inserting a low dielectric constant SiO_2 buffer layer underneath the electrodes.

The microwave effective index n_{eff}, the attenuation constant α (dB/cm), and the characteristic impedance Z (Ω) of the CPW in Fig. 2 have been computed versus frequency, with the present approach (QS-FEM) and with the full-wave technique (FW-FEM) [3]. The results are shown in Fig. 3. The gold electrode conductivity is $\sigma = 4.1 \times 10^7$ S/m. The relative permittivities of the Z-cut X-propagating $LiNbO_3$ substrate are 28 and 43 perpendicular and parallel to the substrate surface, respectively, and the lithium niobate loss tangent is $\tan\delta_s = 0.004$. The relative permittivity of the SiO_2 buffer layer is $\epsilon_r = 3.90$, and the loss tangent is $\tan\delta_b = 0.016$.

An excellent agreement may be observed between quasi-static analysis, the full-wave solution [3], and the results presented in [5]. The small discrepancies, arising at higher frequencies between the quasi-TEM model and full-wave solutions, are related to the onset of higher-order substrate modes. The electromagnetic behaviour of the waveguiding structure is accurately represented with $Q = 8$ problem-matched basis functions, over a bandwidth of 100 GHz.

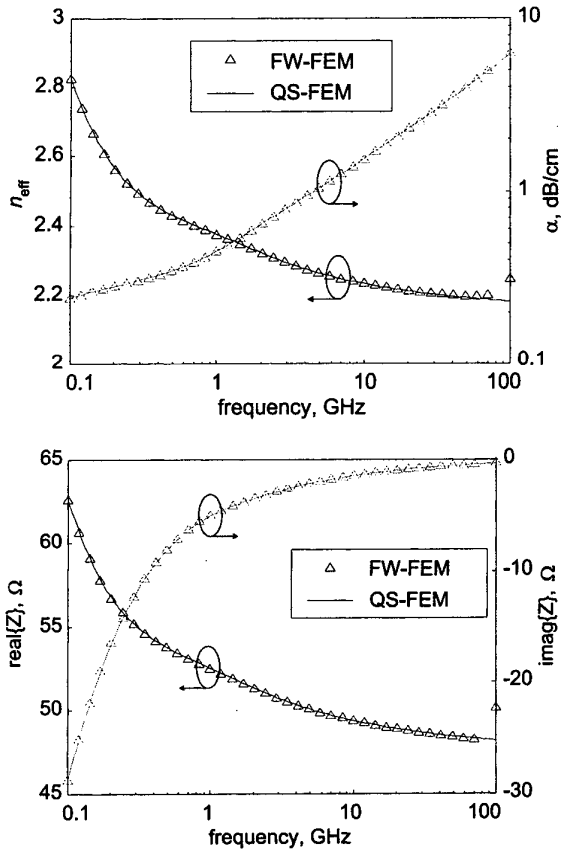

Fig. 3. (a) Microwave effective index n_{eff}, attenuation α (dB/cm) and (b) characteristic impedance Z_c (Ω) of the ridge-type CPW of Fig. 2 , computed with the full-wave FEM approach (FW-FEM), and the present magneto-quasi-static model (QS-FEM).

VI. Conclusion

We have developed a FEM-based fast and accurate reduced-order model for the computation of the frequency-dependent characteristic parameters of lossy inhomogeneous transmission lines. In contrast with conventional quasi-TEM approaches, the present technique is able to capture the electromagnetic behaviour of the waveguiding structure from the low-frequency RC range to the skin-effect LC regime. Excellent agreement with full-wave methods is achieved, at a fraction of their computational cost.

References

[1] R. D. Graglia, D. R. Wilton, and A. F. Peterson, "Higher order interpolatory vector bases for computational electromagnetics," *IEEE Trans. Antennas Propagation*, vol. TAP-45, no. 3, pp. 329–342, Mar. 1997.

[2] F. Bertazzi, M. Goano, and G. Ghione, "Fast higher-order full-wave FEM analysis of traveling-wave optoelectronic devices," in *Proceedings of the 31st European Microwave Conference*, London, Sept. 2001, vol. 1.

[3] F. Bertazzi, O. A. Peverini, M. Goano, G. Ghione, R. Orta, and R. Tascone, "A fast reduced-order model for the full-wave FEM analysis of lossy inhomogeneous anisotropic waveguides," *IEEE Trans. Microwave Theory Tech.*, vol. MTT-50, no. 9, Sept. 2002.

[4] S. V. Polstyanko, R. Dyczij-Edlinger, and J.-F. Lee, "Fast frequency sweep technique for the efficient analysis of dielectric waveguides," *IEEE Trans. Microwave Theory Tech.*, vol. MTT-45, no. 7, pp. 1118–1126, July 1997.

[5] M. Koshiba, Y. Tsuji, and M. Nishio, "Finite-element modeling of broadband traveling-wave optical modulators," *IEEE Trans. Microwave Theory Tech.*, vol. MTT-47, no. 9, pp. 1627–1633, Sept. 1999.

[6] Z. Bai, J. Demmel, J. Dongarra, A. Ruhe, and H. van der Vorst, Eds., *Templates for the Solution of Algebraic Eigenvalue Problems: A Practical Guide*, SIAM, Philadelphia, 2000.

[7] A. Konrad, "Integrodifferential finite element formulation of two-dimensional steady-state skin effect problems," *IEEE Trans. Magn.*, vol. MAG-18, no. 1, pp. 284–292, Jan. 1982.

[8] C. K. Aanandan, P. Debernardi, R. Orta, R. Tascone, and D. Trinchero, "Problem-matched basis functions for moment method analysis—An application to reflection gratings," *IEEE Trans. Antennas Propagation*, vol. AP-48, no. 1, pp. 35–40, Jan. 2000.

[9] S. Ramo, J. R. Whinnery, and T. Van Duzer, *Fields and Waves in Communication Electronics*, John Wiley & Sons, New York, 3rd edition, 1994.

[10] G. I. Costache, "Finite element method applied to skin-effect problems in strip transmission lines," *IEEE Trans. Microwave Theory Tech.*, vol. MTT-35, no. 11, pp. 1009–1013, Nov. 1987.

[11] G. H. Golub and C. F. Van Loan, *Matrix Computations*, John Hopkins Press, Baltimore, 3rd edition, 1996.

[12] G. I. Costache, M. V. Nemes, and E. M. Petriu, "Finite element method analysis of the influence of the skin effect, and eddy currents on the internal magnetic field and impedance of a cylindrical conductor of arbitrary cross-section," in *Canadian Conference on Electrical and Computer Engineering*, Montréal, Sept. 1995, vol. 1, pp. 253–256.

[13] K. Noguchi, H. Miyazawa, and O. Mitomi, "Frequency-dependent propagation characteristics of coplanar waveguide electrode on 100 GHz Ti:$LiNbO_3$ optical modulator," *Electron. Lett.*, vol. 34, no. 7, pp. 661–663, Apr. 1998.

[14] K. Noguchi, O. Mitomi, and H. Miyazawa, "Millimeter-wave Ti:$LiNbO_3$ optical modulators," *J. Lightwave Technol.*, vol. LT-16, no. 4, pp. 615–619, Apr. 1998.